

X-ray absorption

Laboratory and Computational Physics 3
VA Streltsov, CT Chantler,
R Ekanayake, H Melia



Last compiled August 17, 2017

Contents

1	Introduction	3
1.1	Abstract	3
1.2	References	3
2	Part I	4
2.1	Background theory	4
2.1.1	X-ray properties	4
2.2	Production of x-rays. Rotating anode.	8
2.3	Monochromators vs Filters	8
2.4	Basic principle of absorption	10
2.4.1	Physics of x-ray attenuation/absorption* of x-rays by matter	10
2.4.2	Attenuation length	11
2.5	Measuring the mass attenuation coefficient	12
2.5.1	Single component system (a pure material)	12
2.5.2	Multicomponent systems	13
2.5.3	Conclusion	17
2.6	Appendix	18
2.6.1	Derivation of the Beer-Lambert Law	18
2.6.2	Limitations of the Beer-Lambert law	19
3	Part 2	21
3.1	Equipment	21
3.1.1	Radiation used	25
3.1.2	Safety precautions	26
3.1.3	Method	27
4	Experiment 2	29
4.1	Method	29
4.2	Data and Analysis	30
4.3	Conclusions	32

1 Introduction

1.1 Abstract

The aim of this laboratory is to give the student some insight into absorption and attenuation of X-rays by matter and the determination of mass attenuation/absorption coefficients using x-ray spectroscopic measurements. This will involve a thorough investigation into the systematic errors associated with this method and how they must be considered for precise measurements of the atomic absorption factors for metal foils. Working experimental equipment will include a rotating anode, silicon monochromator, and the state-of-the-art Pilatus 100K detector, designed for the detection of x-rays from laboratory and synchrotron sources. X-ray safety, the physics of the rotating anode, silicon crystal, and silicon detector technology will be explored. The first experiment involves setting up the silicon crystal to find the relevant lines of Cu K_{α_1} , K_{α_2} , and K_{β} on the Pilatus detector using a copper rotating anode x-ray source. The second experiment involves measuring the x-ray beam attenuation by Al foils of varying thickness, taking images of the attenuated lines on the Pilatus detector, and using the intensities to explore the Beer-Lambert law. This lab provides an illustrative exemplar of real experiments conducted in the X-ray Optics lab., School of Physics, and at the synchrotrons in the last few years.

1.2 References

- Bunker, G. Introduction to XAFS, Cambridge Press 2010.
- Cullity, B. D. Elements of x-ray Diffraction, Addison-Wesley Publishing Company, Inc. 1956.
- Chantler, C. T. Theoretical Form Factor, Attenuation and Scattering Tabulation for Z=1-92 from E=1-10 eV to E=0.4-1.0 MeV. J. Phys. Chem. Ref. Data 24, 71-643 (1995).
- Chantler, C. T. Detailed Tabulation of Atomic Form Factors, Photoelectric Absorption and Scattering Cross Section, and Mass Attenuation Coefficients in the Vicinity of Absorption Edges in the

Soft X-Ray (Z = 30-36, Z = 60-89, E = 0.1 keV-10 keV), Addressing Convergence Issues of Earlier Work. J. Phys. Chem. Ref. Data 29(4) 597-1048 (2000).

- Chantler, C.T., Olsen, K., Dragoset, R.A., Chang, J., Kishore, A.R., Kotochigova, S.A., and Zucker, D.S. (2005), X-Ray Form Factor, Attenuation and Scattering Tables (version 2.1). [Online] Available: <http://physics.nist.gov/ffast>
- International Tables for X-ray Crystallography [Volume C], 1995 et seq.
- X-Ray Data Booklet from Lawrence Berkeley National Laboratory, Berkeley, CA (for a free copy of the X-Ray Data Booklet go to <http://xdb.lbl.gov/>)
- Mass absorption coefficients and other X-ray related element properties, see <http://www.csrrri.iit.edu/periodic-table.html>

2 Part I

2.1 Background theory

2.1.1 X-ray properties

X-radiation is a form of electromagnetic radiation. X-rays have a wavelength in the range of below 0.01 nm to 10 nm, corresponding to energies in the range 120 eV to over 120 keV. Although γ -rays may have energy in the same range, γ -radiation comes from an excited nucleus and nuclear transitions and decays whilst x-rays are produced by changing electron wavefunction energies - i.e. generally atomic in origin. Because of Heisenberg's uncertainty principle, since the lifetime of nuclear states is generally much longer than that of electronic excited states, the primary physical difference between γ -ray and x-ray photons of the same energy is the lifetime and therefore the energy width of the transition, $\Delta E \Delta t = h/2\pi$

High energy photons are emitted when a solid target is bombarded with

electrons of energy in the range from tens to hundreds keV. Two types of emission are observed. The first, known as bremsstrahlung (literally braking radiation in German), is a broadband or polychromatic radiation produced when the electrons have their velocities changed in magnitude or direction near the nuclei of the atoms of the target. These inelastic collisions with the Coulomb field of nuclei involve the loss of any fraction of the electron kinetic energy. The bremsstrahlung spectrum (white radiation) extends over a wide range of energies from the minimum, almost zero energy photons, to the maximum energy corresponding to that of the incident electron. The maximum energy lost, $E(\max)$, determines the shortest wavelength, $\lambda(\min)$, that can be obtained according to the equation

$$E = eV = \frac{hc}{\lambda} \quad (1)$$

where e is the charge on the electron, V is the accelerating voltage, h is Planck's constant, and c is the speed of light. A more practical form of this equation is given by

$$\lambda = \frac{12.398[\text{\AA}kV]}{V[kV]} \quad (2)$$

where V is in kilovolts and λ is in Ångstroms ($1 \text{ \AA} = 0.1 \text{ nm}$). Thus, the higher the accelerating voltage of the x-ray generator, the shorter the minimum wavelength that can be obtained. The maximum in the intensity of the white radiation occurs at a wavelength that is roughly $1.5 \times \lambda_{\min}$. Longer wavelengths are obtained by multiple-collision processes.

The total intensity, I_w of the white radiation is approximately proportional to the filament current, i , the atomic number of the anode target, Z , and the square of the accelerating voltage, V .

The electron bombardment can instead eject inner electrons from the target atoms leaving a vacancy. This is the second type of transition causing discrete lines in the X-ray spectra. Outer electrons then de-excite into the vacancy producing photons of defined energy - a line emission. The combined spectrum has these characteristic peaks superimposed on the bremsstrahlung base. An increase in voltage above the critical voltage increases the intensities of the characteristic lines relative to the continuous spectrum but does not change their wavelengths (x-ray photon energy). The exact shape of the spectrum of the emitted

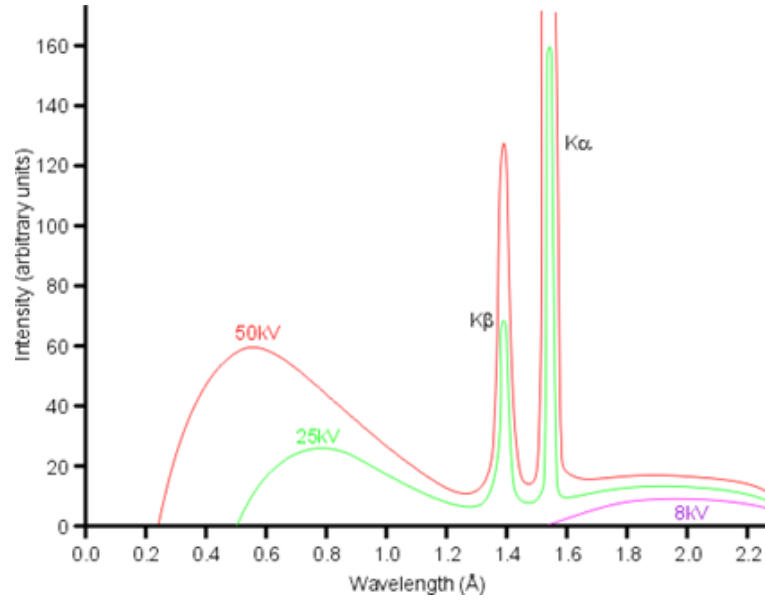


Figure 1: X-ray radiation spectra for electrons of various energies (accelerating voltage) bombarding copper target.

x-ray radiation depends on the energy of the incident electrons, material and thickness of the target, and absorption of the produced x-rays inside the target and by the filter or monochromator usually used at x-ray output. Measured x-ray spectra for copper target are shown in Fig. 1.

According to Bohr's theory, electrons with principal quantum number n have a binding energy in the atom of

$$E_n = -\frac{Z^2 R_e}{n^2} \quad (3)$$

where Z is the atomic number and $R_E = 13.57$ eV is the Rydberg constant. $n = 1$ is the K shell ($1s$ electrons), $n = 2$ is the L shell ($2s, 2p$ electrons), $n = 3$ is the M shell ($3s, 3p, 3d$ electrons) etc. Figure 2 shows the energy-level diagram of a copper atom.

Characteristic X-radiation that is produced following a transition from the L shell to the K shell is called K_α radiation, while the radiation that is produced following a transition from the M shell to the K shell is called K_β radiation ($M_1 \rightarrow K$ and $L_1 \rightarrow K$ transitions are not allowed due to quantum-mechanical selection rules). $\Delta l = \pm 1$ and $\Delta j = 0, \pm 1$ selection rules for the dipole radiation ($l =$ orbital angular momentum, $j =$ total angular momentum).

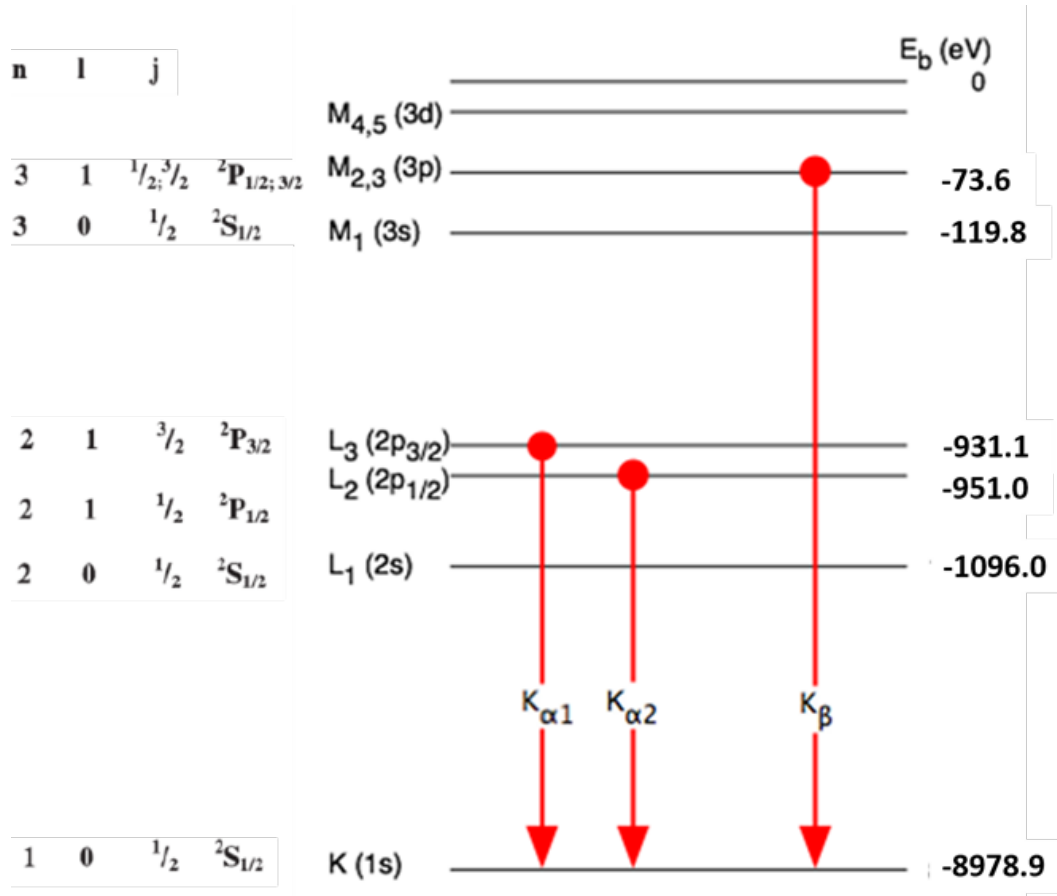


Figure 2: Atomic levels involved in copper K_α and K_β emission.

The characteristic X-ray lines of copper have the following energy levels (Fig. 2):

$$E_{K_{\alpha^*}} = E_K - \frac{1}{2}(E_{L2} + E_{L3}) = 8.038 \text{ keV} \quad (4)$$

$$E_{K_\beta} = E_K - E_{M2,3} = 8.905 \text{ keV} \quad (5)$$

$E_{K_{\alpha^*}}$ is the weighted mean of the K_{α_1} and K_{α_2} line energies.

The energies of x-rays roughly scale with Z^2 , although shielding of the nucleus by other electrons (which happen to be closer to the nucleus at the time) often results in the proportionality being closer to $(Z - \sigma)^2$ where $\sigma \sim 1.2$ for $n = 1$. The energy gained by an electron dropping from the second shell to the first may be reasonably approximated using Moseley's law for K lines:

$$E = R_E(Z - 1)^2 \left(\frac{1}{1^2} - \frac{1}{2^2} \right) = 10.2(Z - 1)^2 \text{ eV} \quad (6)$$

We use an x-ray tube with rotating copper anode to produce copper K

characteristic spectrum in this laboratory.

2.2 Production of x-rays. Rotating anode.

Inside every x-ray tube there is a cathode and an anode. The cathode receives incoming electrical current from the machine's generator and emits a beam of electrons onto the anode. During operation, a large disk-shaped copper anode is rotated at high speed (3000 to 9000 revolutions per minute). The motive force for the rotation is provided by an induction motor the windings of which are housed outside the tube. Although the focal spot of the electrons impinging on the anode is no larger than that in a tube with a stationary anode, the effective area of the anode exposed to the beam is much larger. By this means, the heating of the anode is reduced and the tube loading can be increased (e.g., up to 500 mA with a 2 mm x 2 mm focal spot). The result is a higher intensity of x-rays produced. Rotating anode generators are expensive and require high maintenance but are the most powerful laboratory x-ray source available - any higher x-ray fluxes require a synchrotron.

2.3 Monochromators vs Filters

Many x-ray diffraction and absorption spectroscopy experiments require radiation which is as monochromatic as possible. However, the beam from an x-ray tube operated at a voltage above V_K contains not only the strong K_α line but also the weaker K_β line and the continuous spectrum.

Historically, x-ray filters were used to reduce the unwanted white radiation from the X-ray source and to minimise the K_β radiation. The intensity of these undesirable components can be decreased relative to the intensity of the K_α line by passing the beam through a filter made of a material whose K absorption edge lies between the K_α and K_β wavelengths of the target metal. Such a material will have an atomic number 1 or 2 less than that of the target metal (e.g. Ni ($Z = 28$) for a Cu ($Z = 29$) target). The drawback of filters is that the background radiation is still high and the transmitted radiation is still not very monochromatic.

A more selective and advanced way to produce a beam of radiation with

a narrower wavelength distribution is by using single-crystal monochromators and X-ray diffraction. In practice 'single crystals' are made up of lots of little crystal blocks all approximately aligned in the same orientation to form a mosaic. The distribution of the alignment of the blocks is called the mosaic spread of the crystal.

If a single crystal is set to reflect the strong K_{α} component of the general radiation from an X-ray tube and this reflected beam is used as the incident beam in experiment. Crystal monochromators make use of the periodicity of 'perfect' crystals to select the desired photon energy from a range of photon energies. This is described by Bragg's law:

$$2d_{hkl} \sin \theta = n\lambda \quad (7)$$

where d_{hkl} is the spacing between the planes having Miller indices hkl , θ is the angle of incidence, n is the order of a particular reflection ($n=1, 2, 3\dots$), and λ is the wavelength.

The highest level of monochromatic radiation for a diffraction or absorption experiment is radiation which has itself been diffracted, minimising the energy width of the broadening. All atomic energy levels have a finite width, and emission from these levels is therefore spread over a finite energy range. Indeed, greater monochromaticity is generated by using perfect crystal diffraction, higher order diffraction conditions, and double-crystal diffraction (monochromation).

It is common for two single-crystal monochromators to be connected in series, with their mechanical systems operating in tandem so that they both select the same wavelength. Such double crystal monochromator (DCM) uses two parallel crystals in a (+, -) configuration to produce a monochromatic exit beam which is running parallel to the incident white x-ray beam. Slight detuning the second crystal of the DCM is used to suppressed high-order harmonics in x-ray radiation. A (+, +) configuration can also be used, or the two crystals can be formed from a single monolithic crystal as designed in the X-ray laboratory.

In this laboratory we use a diffracted-beam monochromator consisting of a Si (silicon) DCM mounted on the goniometer and a detector at the 2θ angle from the incident beam direction. Such a device rejects the unwanted K_{β} radiation with little change in the magnitude of the K_{α_1} and K_{α_2} lines or vice versa.

Questions

1. Calculate the wavelength of the copper K series lines (Cu K_{α_1} , K_{α_2})

and K_{β} lines) using the Bohr model of the atom. Explain the differences from the measured values (Cu $K_{\alpha_{1,2}} = 1.541874 \text{ \AA}$ and Cu $K_{\beta} = 1.392250 \text{ \AA}$). Recalculate the wavelengths using the modified model with screening (Moseley's law) and compare with the experimental values.

2. What is the minimum potential (voltage) in V_K that is required to excite Cu K-series radiation from a Cu-target x-ray tube? Calculate excitation voltages (V_K) for Cu K-series and compare with measured absorption edge of Cu ($\lambda = 1.3808 \text{ \AA}$).
3. Calculate the Bragg angles (θ) for a silicon monochromator [111] (the largest d spacing which is from the (111) planes is 3.136 \AA) to satisfy the diffraction conditions for Cu K_{α_1} , Cu K_{α_2} and Cu K_{β} radiation (measured values Cu $K_{\alpha_1} = 1.540598 \text{ \AA}$, Cu $K_{\alpha_2} = 1.544426 \text{ \AA}$, and Cu $K_{\beta} = 1.392250 \text{ \AA}$).

2.4 Basic principle of absorption

2.4.1 Physics of x-ray attenuation/absorption* of x-rays by matter

X-rays are attenuated as they pass through matter. That is, the intensity of an x-ray beam decreases the farther it penetrates into matter. Basically, X-ray photons are absorbed by the electrons of the atom of the material, decreasing the propagating X-ray intensity. The decrease in intensity of the X-ray beam depends upon two factors:

- The depth of penetration (t) or thickness
- An intrinsic characteristic of the material namely the attenuation/absorption¹ cross-section, $\sigma = uM\mu$, (barns per atom)

where u is the atomic mass unit (1.67377×10^{-27} kilogram (kg) = 1/12 of the mass of an atom of the nuclide ^{12}C), and M is the relative atomic mass of the target element, and μ is the linear attenuation/absorption coefficient or the mass attenuation/absorption coefficient $[\mu/\rho]$ - the quantity usually encountered in tabulations of material properties. These

¹Strictly speaking, attenuation and absorption have two clearly different meanings. Attenuation = loss of beam, which may include scattering = redirection of beam and/or loss of partial energy. Absorption = transfer of all photon energy to a particle [electron or whatever], mainly photoelectric effects.

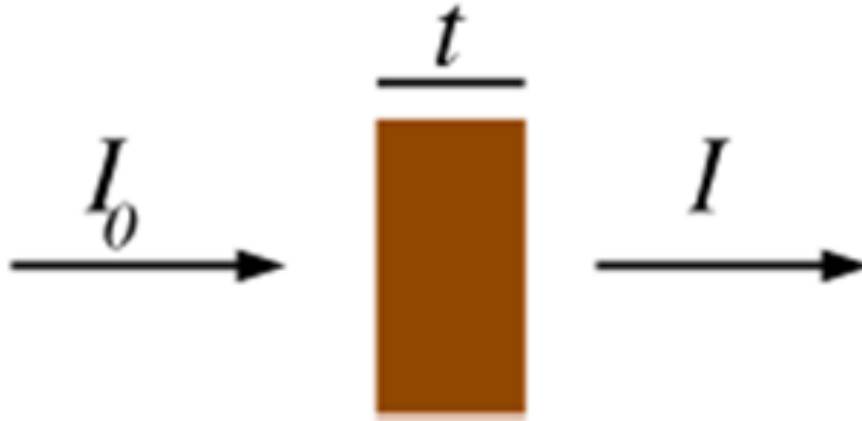


Figure 3: Schematic of incident and transmitted x-ray beam.

two coefficients are related by the density of the material ρ as $[\mu/\rho]\rho = \mu$.

The intensity decreases exponentially with the distance travelled (Fig. 3), or $I(t) = I_0 e^{-\mu t}$, where I_0 is the initial x-ray beam intensity. This exponential decay of photon intensity applies in the optical region of the electromagnetic spectrum as well and was originally defined for optical photon attenuation. It is known as the Beer-Lambert law (see derivation in Appendix).

$$I(t) = I_0 e^{-[\mu/\rho]\rho t} \quad (8)$$

2.4.2 Attenuation length

An interesting application of this equation is to determine the depth of penetration of x-rays. The attenuation length is defined as the depth into the material where the intensity of the x-rays has decreased to about 37% ($1/e$) of the value at the surface. That is, when $I = (1/e)I_0$, or $I/I_0 = 1/e$. [Recall that e , sometimes called Euler's number or Napier's constant, is the base of natural logarithms, or $e \approx 2.7183$.] Then, substituting into equation 8, we get:

$$I/I_0 = e^{-[\mu/\rho]\rho t_1} \quad (9)$$

$$\ln(1/e) = (-[\mu/\rho]\rho t_1) \quad (10)$$

$$-1 = (-[\mu/\rho]\rho t_1) \quad (11)$$

$$t_1 = 1/([\mu/\rho]\rho) \text{ or } t_1 = 1/\mu \quad (12)$$

This also is referred to as the mean free path of the x-rays. For example, given a copper source of x-rays with an energy of 8 keV, how far do these penetrate a piece of pure aluminium (Z=13)? The tabulated (NIST/Chantler) mass absorption coefficient for aluminium from FFAST (<http://physics.nist.gov/PhysRefData/FFast/html/form.html>) at 8 keV is $[\mu/\rho] = 50.33 \text{ cm}^2/\text{g}$. The density of aluminium $\rho = 2.70 \text{ g/cm}^3$. Plugging in the numbers, we find the mean free path $t_1 = 0.007 \text{ cm} = 0.07 \text{ mm} = 70 \mu \text{ m}$.

2.5 Measuring the mass attenuation coefficient

2.5.1 Single component system (a pure material)

We need a source of x-rays — an x-ray tube, for example — and a detector such as a Geiger counter. Place a piece of foil of thickness t_1 between the source and detector and measure the radiation intensity I_1 , as shown in Fig. 3. Now place a second piece of foil with a thickness t_2 in the path and measure the new intensity I_2 . If the original beam intensity is I_0 , then we can write

$$I_1 = I_0 e^{-[\mu/\rho]\rho t_1} \quad I_2 = I_0 e^{-[\mu/\rho]\rho t_2} \quad (13)$$

Dividing these equations,

$$(I_1/I_2) = \frac{e^{-[\mu/\rho]\rho t_1}}{e^{-[\mu/\rho]\rho t_2}} \quad (14)$$

or

$$[\mu/\rho] = \ln(I_1/I_2)/\rho(t_2 - t_1) \quad (15)$$

For example, we use an x-ray tube run at 35 kV and a 0.025-mm thick piece of copper foil. With one foil thickness, our Geiger counter measures 185,000 counts per minute (cpm). When the foil is doubled and the measurement repeated, we find a count rate of about 155,000 cpm. The density of copper is 8.94 g/cm^3 . Then

$$[\mu/\rho] = \frac{\ln(185,000/155,000)}{(8.94 \text{ g/cm}^3)(0.005 \text{ cm} - 0.0025 \text{ cm})} \quad (16)$$

or,

$$[\mu/\rho] = 7.9 \text{ cm}^2/\text{g} \quad (17)$$

The accepted value for the mass absorption coefficient of copper at this energy is approximately $7.0 \text{ cm}^2/\text{g}$. This is a reasonable agreement given the rather crude experimental set-up in which the Geiger counter used had a low-resolution analogue readout meter. We can do quite a bit better than that...

2.5.2 Multicomponent systems

When a sample contains more than one component, the total mass absorption coefficient is the sum of the individual coefficients, each multiplied by the weight fraction present:

$$[\mu/\rho]_s = \sum_i C_i [\mu/\rho]_i. \quad (18)$$

Let's consider an alloy containing 70% Ni and 30% Mo. What is the mass absorption coefficient of this sample at an excitation energy of 22.1 keV (109Cd radioisotope emission)?

For nickel: $[\mu/\rho] (22.1 \text{ keV}) = 23.8 \text{ cm}^2/\text{g}$

For molybdenum: $[\mu/\rho] (22.1 \text{ keV}) = 61.9 \text{ cm}^2/\text{g}$

Therefore,

$$[\mu/\rho]_s = (C_{Ni})([\mu/\rho]_{Ni}) + (C_{Mo})([\mu/\rho]_{Mo}) \quad (19)$$

$$= (0.7)(23.8) + (0.3)(61.9) \quad (20)$$

$$= 35.3 \text{ cm}^2/\text{g} \quad (21)$$

Energy dependence of the mass absorption coefficient and absorption "edges"

The Beer-Lambert law relates strictly only to photoelectric absorption, excluding coherent (Rayleigh, Thomson) and incoherent (Compton diffusion, partial loss of energy and change of direction) scattering, fluorescence, Auger electron and electron pair creation, and other photonuclear reactions within the absorber (Fig. 4).

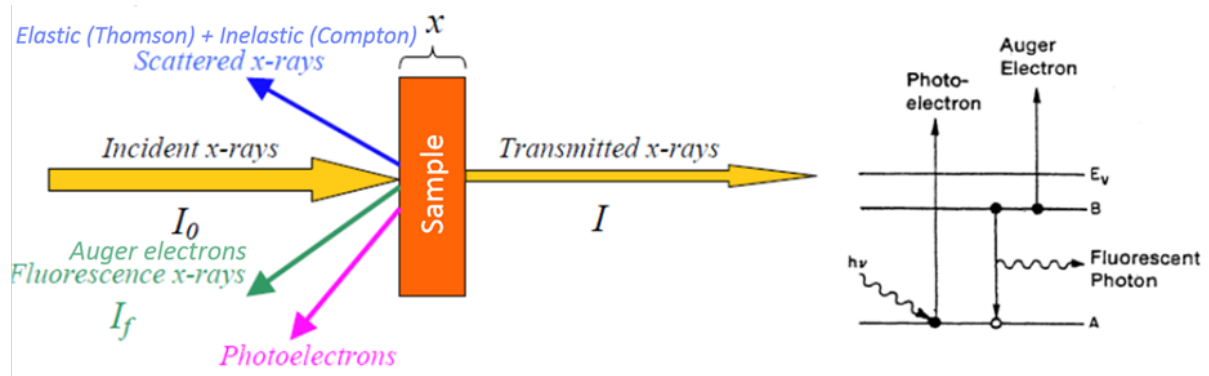


Figure 4: Schematic of interactions of an X-ray beam with matter.

Over large lower energy regions (< 0.5 MeV) and in high- Z materials, the photoelectric effect is predominant and $[\mu/\rho](E)$ is a smooth function of the photon energy, varying approximately as $[\mu/\rho](E) \sim \rho Z^4/(mE^3)$ (an empirical relation is sometimes: $[\mu/\rho](E)_{pe} \sim Z^{4.5}/E^{3.5}$). Here ρ denotes the sample density while Z and m are the atomic number and mass, respectively. The strong dependence of $[\mu/\rho]$ on both Z and E is a fundamental property of X-rays, and is the key to why X-ray absorption is useful for medical and other imaging techniques including X-ray computed tomography (CT). Due to the Z^4 dependence, the absorption coefficient for O, Ca, Fe, and Pb are very different - so that good contrast between different materials can be achieved.

At very low photon energies ($<$ hundreds of keV), Rayleigh scattering is the main scattering process when a photon can also scatter from an atom as a whole, neither exciting nor ionising the atom. Rayleigh scattering is important for visible light and is responsible for the blueness of the sky and depends on the inverse square of initial photon energy, $[\mu/\rho](E) \sim E^{-2}$. At very high energy ($\gg 1$ MeV), $[\mu/\rho]$ is proportional to Z due to a dominance of [nuclear] electron pair creation. However, in the intermediate energy range from hundreds of keV to several MeV, the Compton effect is important, $[\mu/\rho]$ is almost independent of Z and decreasing as the photon energy increases ($\sim Z \ln E/E$ at high energies $E > 0.5$ MeV). It is most often the predominant interaction mechanism for γ -ray energies typical of radioisotope sources. It is the most dominant interaction mechanism in tissue.

In the energy range of our X-ray experiments (8 keV), the scattering (coherent and incoherent) contribution is small but should be taken in to

account as a sum of separated mass attenuation coefficients:

$$[\mu/\rho]_{tot} = [\mu/\rho]_{pe} + [\mu/\rho]_{scatt} \quad (22)$$

where $[\mu/\rho]_{tot}$ - total mass attenuation coefficient, $[\mu/\rho]_{pe}$ - mass absorption coefficient due to photoelectric effect, and $[\mu/\rho]_{scatt}$ - mass attenuation coefficient due to coherent and incoherent scattering. These two contributions vary with energy in different ways. The values can be obtained from the US reference tables:

<http://physics.nist.gov/PhysRefData/FFast/html/form.html>

Note, $[\mu/\rho](E)$ decreases with increasing photon energy. If the latter equals or exceeds the binding energy of a core electron, however, a new absorption channel is available in which the photon is annihilated thereby creating a photoelectron and a core-hole. This leads to a sharp increase in absorption coefficient as shown schematically in Fig. 5. This near-discontinuity in the mass absorption coefficient is called an 'absorption edge'. Above the absorption edge, the difference between the photon energy and the binding energy is converted into the kinetic energy of a photoelectron and $[\mu/\rho](E)$ continues to decrease with increasing photon energy. After a short time of the order of 10-15 s, the core-hole is filled by an electron from a higher energy state. The corresponding energy difference is released mainly via fluorescence X-ray or Auger electron emission (Fig. 5).

Fig. 6 presents the energy dependence of the mass absorption coefficient of Lead (Pb) in a traditional log-log format.

The edges are named according to the principle quantum number of the electron that is excited: K for $n = 1$, L for $n = 2$, M for $n = 3$, etc. The core-electron binding energy increases with increasing atomic number, ranging from 284 eV for the C K-edge to 115,606 eV for the U K-edge, with the L-edges at significantly lower energies than the corresponding K-edge (e.g., 270 eV for the Cl L1-edge, 20,948 eV and 17,166 eV for the U L2- and L3-edges).

Closer examination of Fig. 6 (see inset) shows that the L-edge is in fact three distinct L- edges, named L1, L2, and L3 in order of decreasing energy. L1 corresponds to excitation of a 2s electron. The 2p excitation is split into two edges, L2 and L3, as a consequence of the spin-orbit coupling energy of the 2p⁵ configuration that is created when a 2p electron is excited. The higher energy of the 2p⁵ excited states is the 2P_{1/2} term; This gives rise to the L2 edge. At lower energy is the L3-edge, corresponding to the 2P_{3/2} excited state. Due to degeneracy, the L3-

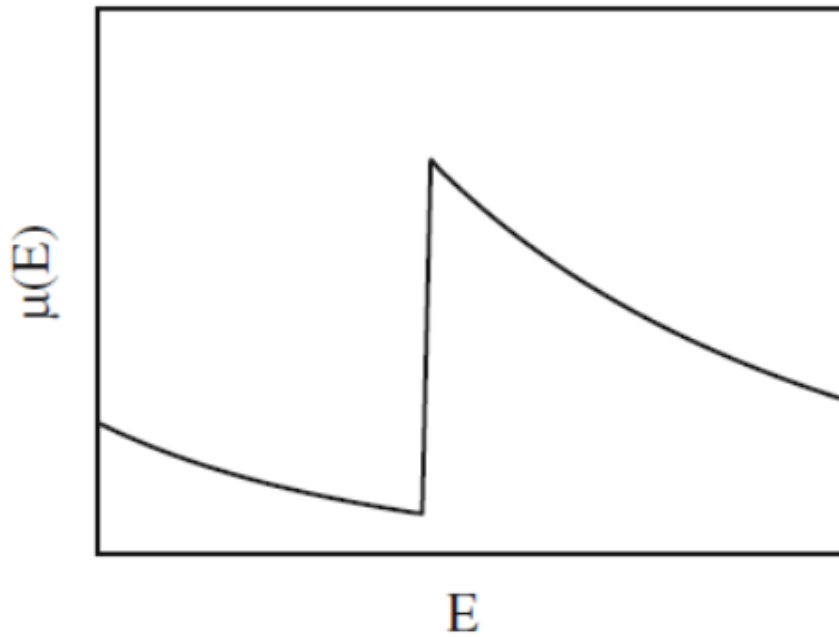


Figure 5: Absorption coefficient $\mu(E)$ versus photon energy E around an absorption edge.

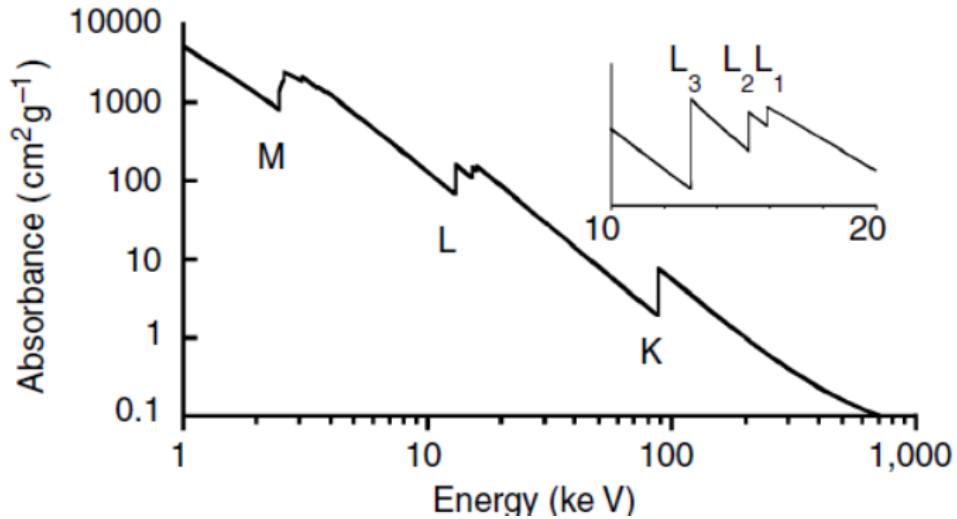


Figure 6: Low-resolution X-ray absorption spectrum for Pb. Three major transitions are seen (K, L, and M edges), corresponding to excitation of an electron from $n = 1, 2,$ and 3 shells, respectively. At higher resolution (inset), the L and the M edges are split.

edge has twice the edge jump of the L₂- and L₁-edges. In contrast with valence electron shells where spin-orbit coupling energies are relatively

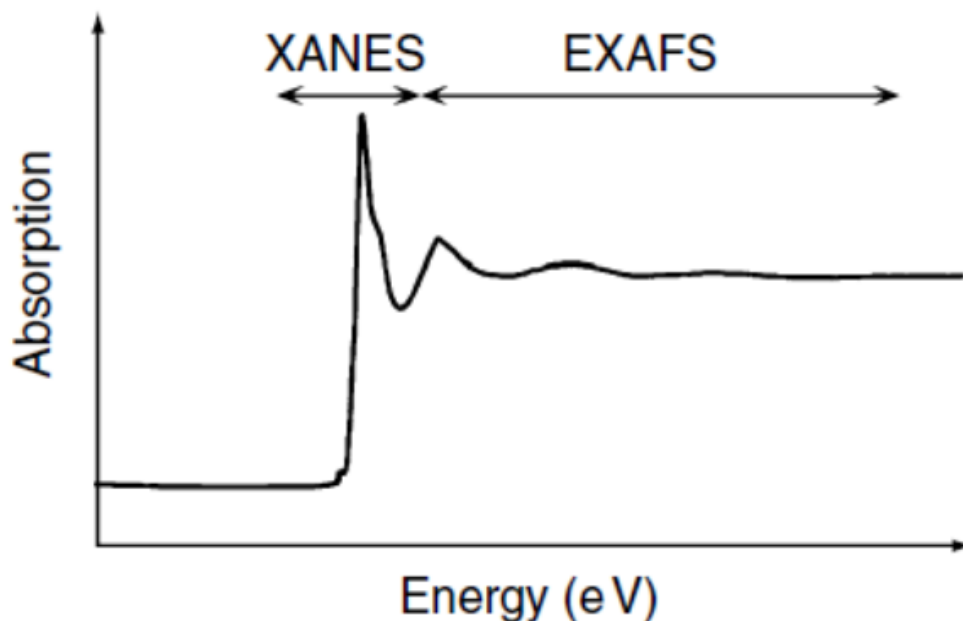


Figure 7: Schematic illustration of an x-ray absorption spectrum, showing the structured absorption that is seen both within ca. 50 eV of the edge (the XANES = X-ray Absorption Near Edge Structure) and for several hundred to >1,000 eV above the edge (the EXAFS = Extended X-ray Absorption Fine Structure).

small, the spin-orbit coupling for core shells can be quite large. For Pb, the L2-L3 splitting is 2,165 eV (1 eV = 8,066 cm⁻¹). Analogous, albeit smaller, splitting occurs for the lower energy edges, with 5M edges, 7N edges etc. X-ray absorption spectroscopy (XAS) refers to the measurement of the energy dependence of mass absorption coefficient $[\mu/\rho]$ in the vicinity of one or more absorbing edges (electron binding energies) (Fig. 7).

2.5.3 Conclusion

The attenuation of x-rays by matter is a specific example of the more general phenomenon of the attenuation of electromagnetic radiation by matter. In the optical region of the electromagnetic spectrum, this phenomenon finds significant spectrometric application in the form of the Beer-Lambert law. This attenuation is characterized by the mass attenuation coefficient of the matter, an important consideration in x-ray absorption spectrometry (XAS).

Questions

1. Plot the ratio of transmitted to incident intensity vs. thickness of aluminium sheet for Cu K_{α} radiation and a thickness range of 0.00 to x (e.g. 0.2) mm.
2. Calculate the mass $[\mu/\rho]$ and linear (μ) absorption coefficients of air for Cu K_{α} radiation. Assume that air contains 80 percent nitrogen and 20 percent oxygen by weight, with a density of 1.29×10^{-3} gm/cm³. Plot the transmission factor of air for Cu K_{α} radiation and a path length of x (e.g. 20) cm.
3. A sheet of aluminium 1 mm thick reduces the intensity of a monochromatic x-ray beam to 23.9 percent of its original value. What is the wavelength of the x-rays?

2.6 Appendix

2.6.1 Derivation of the Beer-Lambert Law

The Beer-Lambert law (or Beer's law, August Beer - German physicist) is the linear relationship between absorbance and thickness (or concentration) of an absorbing species.

1. The number of photons absorbed ΔI in a given thickness Δt is proportional to the incident intensity I_0 and the thickness: ΔI proportional to $-I_0 \Delta t$, where the minus sign indicates a decreasing intensity with thickness.
2. Let A be the constant of proportionality, the absorption coefficient, and we can write $\Delta I = -A I_0 \Delta t$
3. Letting the Δ become infinitesimally small, we have, in differential notation, $dI = -A I_0 dt$
4. Integrating from $t = 0$ to a depth t, we get $I = I_0 e^{-At}$, where I_0 is the initial intensity at $t = 0$.

2.6.2 Limitations of the Beer-Lambert law

The linearity of the Beer-Lambert law is limited by fundamental, chemical and instrumental factors. Including both the X-ray and optical regions of electromagnetic spectrum, causes of nonlinearity include: Fundamental

- any coherent elastic scattering - that is, any elastic scattering where the interaction between atoms or molecules is not independent. It may be 100% positively correlated (Bragg-Laue peaks) or close to 100% destructive (thermal diffuse scattering) and in both cases is non-linear with increasing thickness and number of scatterers
- inelastic scattering where the angular dependence of the scattered radiation interferes with the measurement. The detector orientation will lead to an angular dependence in a non-linear fashion, and to a vector relation.
- any non-monochromaticity from the incident beam, the filter or monochromators, the band-width of the energy incident upon the sample, any harmonic contamination of the beam in the lab source or in the synchrotron beam will lead to a complex function observable with good [advanced] technique
- deviations in absorptivity coefficients at high concentrations ($>0.01M$) due to electrostatic interactions between molecules in close proximity
- scattering of light due to particulates in the sample
- changes in refractive index at high analyte concentration
- fluorescence or phosphorescence of the sample

Chemical

- shifts in chemical equilibria (if the analyte is involved in some equilibrium reaction) as a function of concentration

Instrumental

- detector non-linearities. No detector can ever measure fluxes, intensities, and counts across all possible experimental ranges. If the count or count-rate is too low, dark currents will be recorded in most detectors from the electronics. Cosmic rays may also dominate over the experimental signal. At high count-rates or fluxes,

all detectors have a dead time, or a time required for processing a signal or count, below which counts are either not recorded or are heavily distorted. Understanding the detector, the experimental geometry, the windows and filter materials, enables observation and correction for these effects.

3 Part 2

Experiment 1

Here we are aiming to set up the silicon crystal to find the relevant lines of Cu K_{α_1} , K_{α_2} , and K_{β} on the Pilatus detector using a copper rotating anode x-ray source.

3.1 Equipment

The equipment includes a rotating anode x-ray tube, silicon double crystal monochromator and Pilatus 100K detector. For details of the design and operation of the X-ray Optics Lab machines see the corresponding manuals.

The Rotating Anode preparation and turning on procedures (performed by demonstrator with the help of students)

1. Check if the cooling water is ON: Chiller ON; Water ON.
 - Ball valve in the water line: horizontal - completely closed, vertical - completely open, operating position is 45°.
 - Anode water level: greater than 10 L/min. Tube water level: greater than 5 L/min. Typical values are 12 and 6 L/min, respectively.
 - If both the above conditions are not met, the water ready light will not come on and x-rays will not be produced.
2. Checking if the dry air flow is ON through the transparent tube. This is the outlet of the pump at the back of the machine and keep that tube in the green bucket.
3. Turn vacuum backing pump ON (black button 0 to 1): Pump is under the instrument at the back near the green bucket. You should hear the pump whirring up to speed. The pump needs to come down to the 10⁻² Torr range before turning on the rotating anode turbo pump: wait about 20-30 minutes.

4. Turning ON the rotating anode. Proceed from left to right along the wall to turn ON, and in reverse to turn OFF.
5. Transformer fan power switch (button) to ON.
6. Three-phase power switch (dial switch) to ON.
7. Transformer isolating switch (handle) to ON: 0 to 1.
8. Close all doors: Listen to click sound and confirm from the green bulb on the door; If bulbs don't work properly, then use the reset button in the box next to the cupboard [or replace bulb].

Control Panel of the rotating anode high voltage generator:

1. Follow buttons from left to right; ON = Blue buttons; OFF = Red buttons. Lights must be Ready before turning On.
2. Power to ON: mains power is available when the LINE light is green.
3. Water to ON: READY light green when water is available to the cooling system, check flow rates now.
4. Vacuum Monitor to ON: This turns on the turbo pump on the RA. You should hear the high-pitch frequency, and you should hear the frequency going up as the vacuum pumps down. Initially the backing pump pressure will go up as the turbo pumps the gas evacuated from the anode volume into the backing line. Once turned on, wait for vacuum to come down to a suitable level, ie 3×10^{-7} Torr. This can take several hours or even overnight if the entire system has been completely shut down for a long time. The READY light will go green once the vacuum has been achieved. Using the Anode log sheet to Record the vacuum pressure and other experimental details in the log book.
5. Target to ON: Vacuum value will change suddenly [up] as the anode starts to spin, and some outgassing will occur. Then it will return to the previous value.
6. X-rays to ON: Ready light should be green before turning the x-rays on, Voltage and current should be recorded on the log sheet and in the logbook.
7. Shutter OPEN: Left shutter. Now you have X-rays in the hutch, hitting your experiment. I hope you got it set up first! Also the monitor detector should be on and checking the background outside the hutch at this step.

8. Turning Off the Rotating Anode: Work in reverse of the startup panel steps for daily use, and continue for total shut down.
9. Emergency Stop: Pressing the red emergency button on the left of the RA control panel will shut off all power to the RA control: DON'T USE it unless an emergency. Define Emergency!

Turning on computers and controllers of the goniometer (monochromator) and the Pilatus detector.

Kohzu Controller PC (monochromator)

1. Turn on the PC: it will load Win 98
2. If it asks for the disk, just hit "ok" and "cancel" to ignore
3. Login:
 - username: apayne
 - password: Mellesgriot
4. Open the Kohzu application on the desktop
5. To use Kohzu:
 - always use normal: 0
 - direction can be CW or CCW (clockwise or counterclockwise)
 - angle in degrees: 1 (ie. 1 degree)
 - axis: 0 (to rotate the crystal on the horizontal plane)
 - axis: A = small Cu
 - axis: B = big silver
 - Important! when ask to continue move (rotate):
 - Enter: 1 to continue or
 - Enter: 0 to finish and shut down Kohzu. Never enter letters (like "NO" or anything else), it will rotate monochromator to an arbitrary angle resulting in the loss of alignment to spectral lines.

Pilatus PC (detector)

1. Login:
 - username: det

- password: Pilatus2
2. Change to the p2_det folder where all the programs, start-up files, and logs are stored: `cd p2_det/images/rot_anode/cu/`
 3. Make new directory in which to save any new images that will be taken: `mkdir ./20170921` (for example)
 4. Run TVX: `cd p2_det/, ./runtvx`
 5. This will open the camserver and tvx windows.
 6. As part of the startup process, tvx will then run.

Using TVX

- `imagepath` shows the current directory.
- `imagepath`
/home/det/p2_det/images/rot_anode/cu/... (change to already created directory in which to save images).
- Taking an exposure:
 - Single Exposure: `expose 10` (10 second exposure): If there are no other images in the current folder, the first image will be saved as `00000.tif`. Any subsequent images will be saved as `00001.tif`, etc. Likewise, if there were images already saved in the current directory, the image names will continue numbering where the previous images left off.
 - Repeating Exposure: `exposem 1` (1 second exposure): Initiates a loop where an exposure is taken, saved to `temp.tif`, and displayed. Repeats until broken with `esc`.
 - `disp [filename]`. Display an image. Opens up to 3 windows for successive invocations.
- Extra TVX options:
 - Sliders - Control the colour scheme (contrast factor; thermal, spectral, greyscale, etc) of the image, as well as the range of values displayed.
 - Zoom Factor - Size of the selection area.
 - Selector type - Shape of selection area (pointer, box, annulus, butterfly).
 - Any zoom factor other than `x1` will open a separate window

displaying the contents of the selector area, centered on the mouse pointer once clicked.

- Holding the right mouse button on the edge of the selector shape will allow you to move that edge. Alternatively, exact specs can be typed directly into the selector spec fields.
- setdac0
 - * sets all the digital analog converters to the user predefined values in the startup file user.gl.
 - * This is automated, every time tvx is started, any previously input threshold values will be replaced with those in setdac0
- rbd
 - * (read back detector) produces a green image of Pilatus 16 chips.
 - * digital test; loads 1000 counts onto each pixel.
- calibdet
 - * (calibrate detector) produces a blue image of Pilatus 16 chips
 - * analog test; feeds 100 simulated pulses into each pixel
These two tests should always be run on start-up since they verify the functionality of the detector and show any dead or misfiring pixels that may need recalibration. These tests also reveal that one of the chips is completely dead.

3.1.1 Radiation used

The x-ray tube has a copper (Cu) target. The beam from the x-ray tube operated at a voltage above V_K contains not only the strong K_{α_1} line but also the strong K_{α_2} line and weaker K_{β} line. The wavelengths of these lines are given as²:

$$\text{Cu } K_{\alpha_1}, \lambda = 1.5405 \text{ \AA}$$

²Reference: ITC C

$$\text{Cu K}_{\alpha_2}, \lambda = 1.5444 \text{ \AA}$$
$$\text{Cu K}_{\beta}, \lambda = 1.392 \text{ \AA}$$

The used voltage and current (normally 20 kV and 10 mA), filament size, and target (Cu) are shown on the panel of the high voltage generator.

3.1.2 Safety precautions

X-ray beams are very penetrating and can be dangerous. [Note if it is very high energy or very low energy it is less dangerous because it interacts less with the human body, organs and bones. So the very reason X-rays are good and useful is also why you should take proper care.] Rotating anodes can produce the strongest X-ray beams outside of a synchrotron or a free electron laser. Therefore:

1. Check that the radiation monitor is ON and working.
2. Check that the lead-lined sliding doors are correctly in position.
3. You should avoid any unnecessary exposure by keeping away from the sources (r^{-2} dependence) and limit the time of being in proximity to them.
4. Another safety concern is the high voltage power supply used to power on detector. Do not switch on the high voltage power supply if high voltage cables are not connected to the detector. Do not disconnect high voltage cables if the high voltage power supply is active. If you notice any exposed or damaged

electrical wires, please notify laboratory staff immediately.

3.1.3 Method

1. Using calculations above (problem 3 of part 1) for the Bragg angle (θ) of the silicon monochromator to satisfy the diffraction conditions for Cu K_{α_1} radiation, we can set up the silicon crystal to that θ angle and record the relevant lines of Cu K_{α_1} , K_{α_2} , and K_{β} on the Pilatus detector. Note which direction to move to change between Cu K_{α_1} , K_{α_2} , and K_{β} .
2. Calculate the integrated intensities (I) of the peaks from TIFF image files using MatLab or ImageJ and estimate their ratios.
3. Analyse and explain deviations from expected ratio of ($I_{\alpha_1} : I_{\alpha_2} = 2 : 1$).
4. Why is this ratio always 2:1? Can you explain/estimate it using the various quantum numbers of the different shells? (See Fig. 2).

Steps to do the calculations in Matlab

1. Change the directory to the data folder
2. To read the .tif file `A=imread('filename.tif')`
3. To look at tif file `Image(A)`
4. To look at the 1D profile histogram image `S=sum(A)`
5. To look at the profile `plot(S)` (you can see k-alpha1 and k-alpha2)
6. To look at the profile in between two points `plot(S(x:y))` (to zoom in)
7. Find the minimum between K-alpha1 and K-alpha2
8. To get the integrated intensities, get the sum of each peak by summing over the region.
9. Get the ratio of two peaks

Steps to do basic intensity quantification with ImageJ. There are many ways to get intensity information from images using the base package of ImageJ (no plugins required). This is one of them.

1. Analyze -> Set Measurements
2. Check the boxes next to the information you want. You can get information on area, standard deviations as well as information about intensity.
3. Draw a region of interest (ROI) around your object (e.g. a box) with one of the drawing tools. If you have one image to analyze then go to step 5, or do step 4 for multiple images
4. Edit -> Selection -> Restore Selection to copy/paste that area onto another image to analyze the same size/shape area in another image.
5. Analyze -> Measure to get information on the ROI. Results table will be shown in the separate window. In the Results window you can save Results in Excel format for further analysis and plotting
6. File->Save As-> Results.xsl
7. Note: if the image doesn't show spectral lines (black image), then Adjust/Window/Level in ImageJ to see them.

4 Experiment 2

Here we are taking measurements of the mass absorption coefficients for metal foils using X-ray photons

4.1 Method

Our source of monochromatic x-rays are our targets from the characteristic lines described in experiment 1 ($\text{Cu } K_{\alpha_1}$, K_{α_2} , and K_{β}) To measure the attenuation of the X-ray intensity in matter, we placed different thicknesses of Al foils between the source and the detector (Fig. 8).

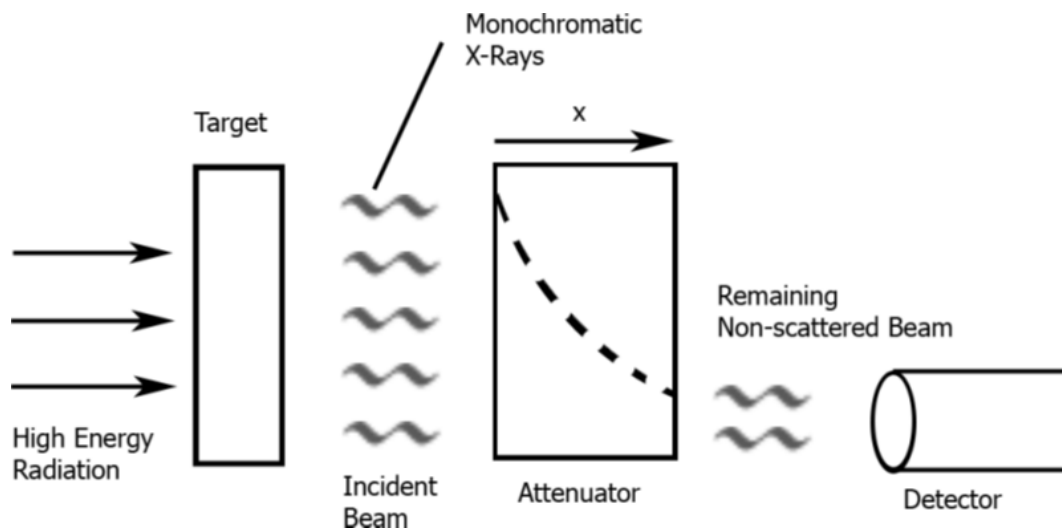


Figure 8: This diagram shows the set-up for our investigation of x-ray scattering cross sections.

In this experiment, we use the following procedures:

1. Mount foils on the goniometer. What thickness do you measure using a micrometer? Estimate your uncertainty.
2. Collect intensity counts (images) at X different thickness values using Pilatus detector.
3. Derive the thicknesses of X foils of Al. Estimate uncertainties in your measurements. Compared with micrometer measurements.

4. Use the reference thickness to determine the mass attenuation coefficient of aluminium for the given energies.

4.2 Data and Analysis

To calculate the thickness of the Al foil and the mass attenuation coefficients and the attenuation cross sections for Cu K_α and Cu K_β radiation from our measured quantities, we used the following method:

1. Obtain values of $[\mu/\rho]$ for both the K_α and the K_β lines using interpolation of values listed on the tabulated (NIST/Chantler) mass absorption coefficient for aluminium from FFAST (<http://physics.nist.gov/PhysRefData/FFast/html/form.html>.)

Take the energy values of E_{α} and E_{β} from the EXPERIMENT 1. Remember from theory notes above that $[\mu/\rho]$ dependence of energy is nonlinear and two contributions vary with energy in different ways. Interpolate all three tables $[\mu/\rho]_{tot}$, $[\mu/\rho]_{pe}$ and $[\mu/\rho]_{scatt}$ and obtained foil thickness using $[\mu/\rho]_{tot}$ from the table and as a sum of two components $[\mu/\rho]_{pe}$ and $[\mu/\rho]_{scatt}$. Compare and analyse results.

2. Obtain an intensity spectrum (TIFF images) for each of the X thickness values (x) plus one additional spectrum for the reference intensity ($I_0, x=0$)
3. Using MatLab or ImageJ (see Experiment 1) find integrated intensities that correspond to the K_α and the K_β lines from recorded detector images.
4. From the intensity spectra, determine at the intensity ratios ($\ln[I(x)/I_0]$) and plot against the number (n) of Al foils of thickness (x) used similar to Fig. 9. The modulus of the slope of the linear fits will give us product of $[\mu/\rho]\rho x$ - the mass attenuation coefficient and the attenuation thickness $x\rho$ (ρ density of material). From this value we found, first, the thickness of the foil using interpolated values of the mass attenuation coefficient $[\mu/\rho]$ at K_α energy.
5. These fits will also give the statistical estimates of the error bars. Explore it in error analysis below.
6. Use calculated values of the Al foil thickness to estimate the

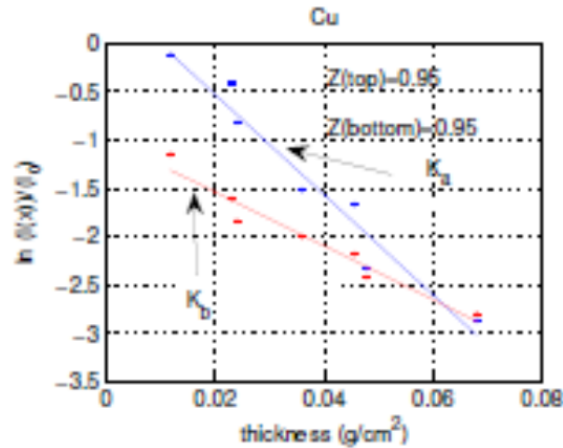


Figure 9: An example of $\ln[I(x)/I_0]$ vs $-\mu \cdot x$ plot.

value and the error of the mass absorption coefficient at K_β energy. Compare this $[\mu/\rho]$ K_β with that interpolated in 1 from the NIST/Chantler table. Estimate errors.

7. In a given material, the probability of photoelectric interactions occurring is strongly dependent on the energy of the photon and its relationship to the binding energy of the electrons, this implies that the mass attenuation coefficient of a material should also be energy dependent. In general, we should expect that μ decreases with increasing energy of the impinging x-rays. Investigate the energy dependence of μ . Since the K_α lines have lower energies than the K_β lines, the μ 's of the K_α lines are greater than those of the K_β lines. This relation implies that if we increase the energy of the incoming x-rays, the x-rays beams will be absorbed less by the barrier matter, and its intensity will also be reduced by a smaller amount.
8. Once we calculate μ for K_α and the K_β energies we can also know the cross section in barns per atom σ from the following relation: $\mu = \sigma/uM$, where u is the atomic mass unit (1.67377×10^{-27} kilogram (kg) = 1/12 of the mass of an atom of the nuclide ^{12}C), and M is the relative atomic mass of the target element.

Error analysis and sources of systematic uncertainty

1. Since in this experiment the number of counts that we collected is on the order of 104, the statistical error bars in a natural log plot are therefore very small.

2. However, we still see some systematic scattering of the dataset around the linear fits. The thickness of the Al foils could contribute to systematic uncertainties in x . Estimate how this would correspond to an uncertainty in μ .
3. The Beer-Lambert law relates strictly to photoelectric absorption excluding other effects in Fig. 4 which may not have been accounted for accurately.
4. Uncertainty in theoretical tables and in the interpolation of table $[\mu/\rho]$ values.

4.3 Conclusions

We confirmed Moseley's Law, at least for the K lines in EXPERIMENT 1 and Beer-Lambert Law in EXPERIMENT 2. We also showed in EXPERIMENT 2 that the values of μ and σ , based on our measurements of X thicknesses of Al foil with energies of Cu-target are close to the reference values within their error bars. Thus, we verified our hypothesis that when a beam of X-ray passes through matter, holding the attenuation thickness constant, the intensity of the beam with higher impinging energies will attenuate less than those with lower energies. A similar relation was also found in the attenuation cross section.